Electronic Supplementary Material (ESI) for Journal of Materials Chemistry B.
This journal is © The Royal Society of Chemistry 2021

Supporting Information

Coacervate microdroplet protocells-mediated gene transfection for nitric oxide production and induction of cell apoptosis

Yanwen Zhang, Yu Yao, Songyang Liu, Yufeng Chen, Shaohong Zhou, Kemin Wang, Xiaohai Yang and Jianbo Liu**

State Key Laboratory of Chemo/Biosensing and Chemometrics, College of Chemistry and Chemical Engineering, College of Biology, Key Laboratory for Bio-Nanotechnology and Molecular Engineering of Hunan Province, Hunan University, Changsha 410082 (P. R. China).
E-mail: liujianbo@hnu.edu.cn, xiaohaiyang@hnu.edu.cn

SI Figures

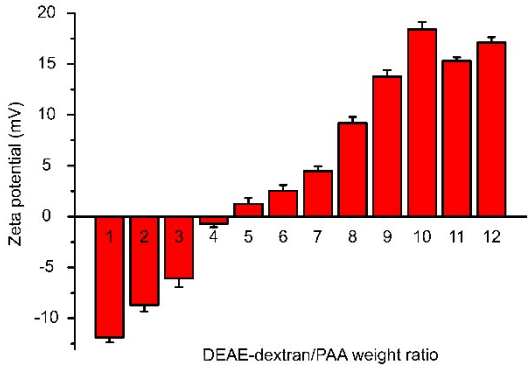

Figure S1. Zeta potential of coacervate microdroplets, prepared from different weight ratios of DEAE-dextran and PAA (1:1-12:1, w/w).

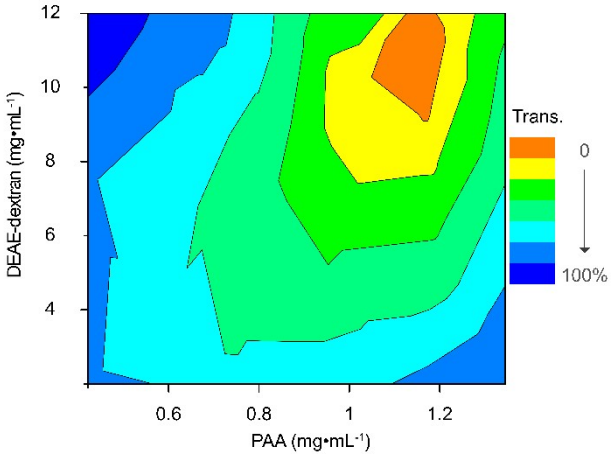

Figure S2. Partial phase diagram for the preparation of DEAE-dextran/PAA coacervate microdroplet via liquid–liquid phase separation. The phase diagram was plot based on optical transmittance (Trans., 420 nm) measurements recorded at different polyelectrolyte concentrations.

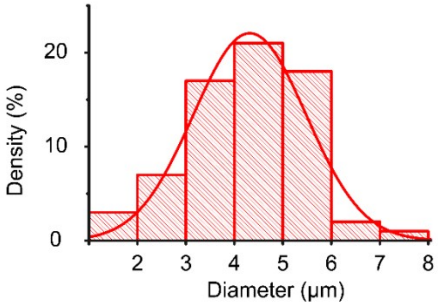

Figure S3. The size distribution of the coacervate microdroplets observed from confocal imaging was analyzed to be 5.4 ±1.5 μm. There are no obvious differences between the statistic result and the DLS result (5.0 ± 1.4 μm). t-test, p=0.545.

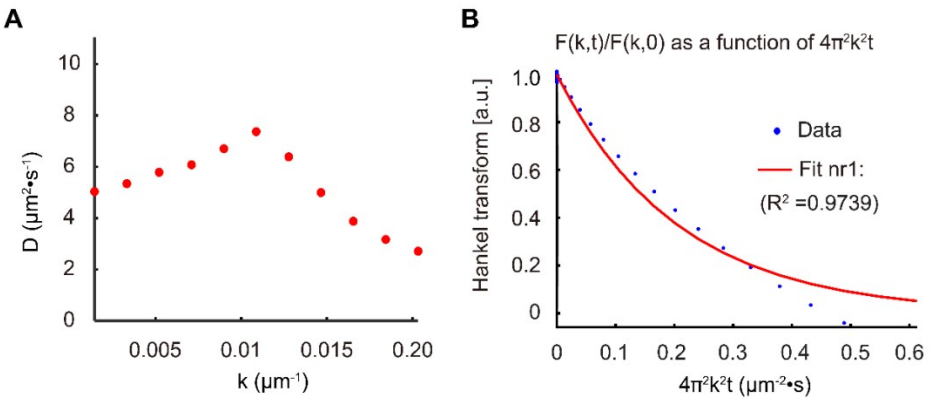

Figure S4. **(A)** Fitting plot showing the diffusion coefficient value of *D* (k) determined at each individual value of k in coacervate protocell. **(B)** Graph showing the curve fit of F(k,t)/F(k,0) vs $4\pi^2k^2t$ in coacervate protocell. The diffusion coefficient was fitted from the curve in **Figure 1E, F**.

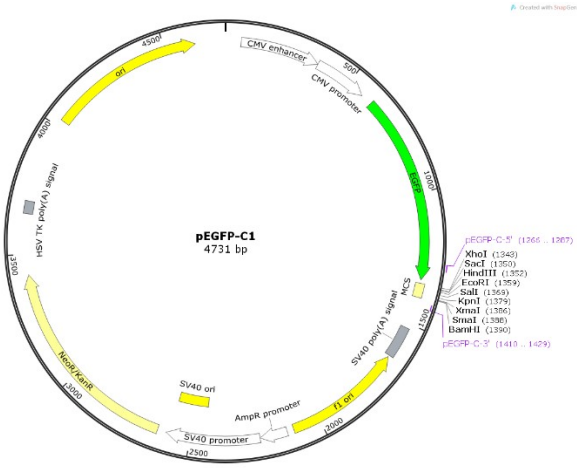

Figure S5. The plasmid profiles of pEGFP-C1.

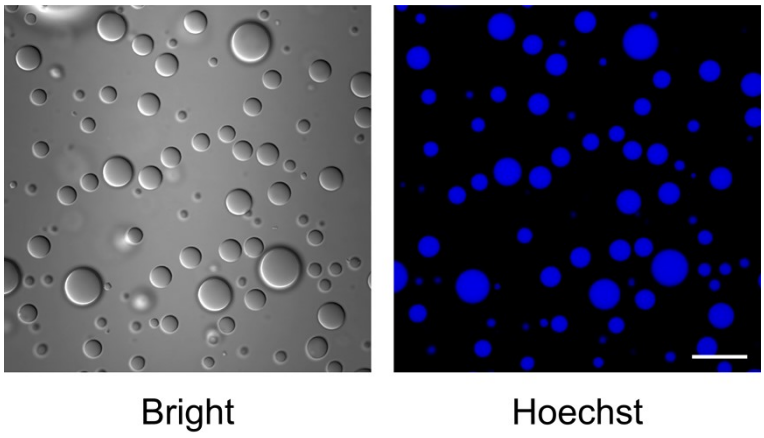

Figure S6. Bright and fluorescent images of the coacervate microdroplets in which pDNA was stained with Hoechst (a blue fluorescent stain for labeling DNA). Scale bar: 10.0 μm.

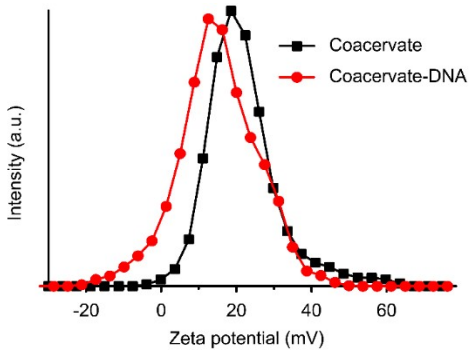

Figure S7. The zeta potential of DEAE-dextran/PAA coacervate microdroplets before (black) and after (red) sequestration of pEGFP.

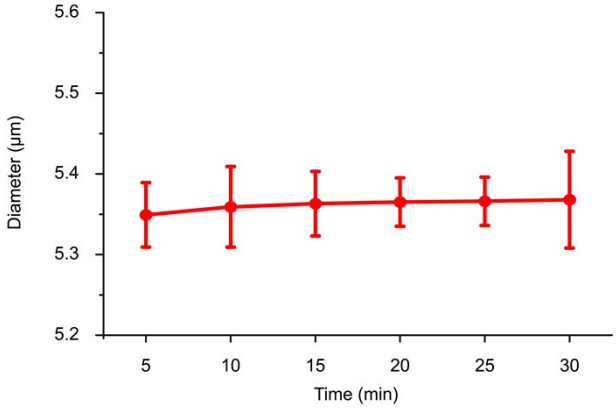

Figure S8. Time-dependent size change of the coacervate microdroplets. Each value is represented as a mean ± standard deviation of 3 samples. The concentration of coacervate microdroplets is 50 ug/mL.

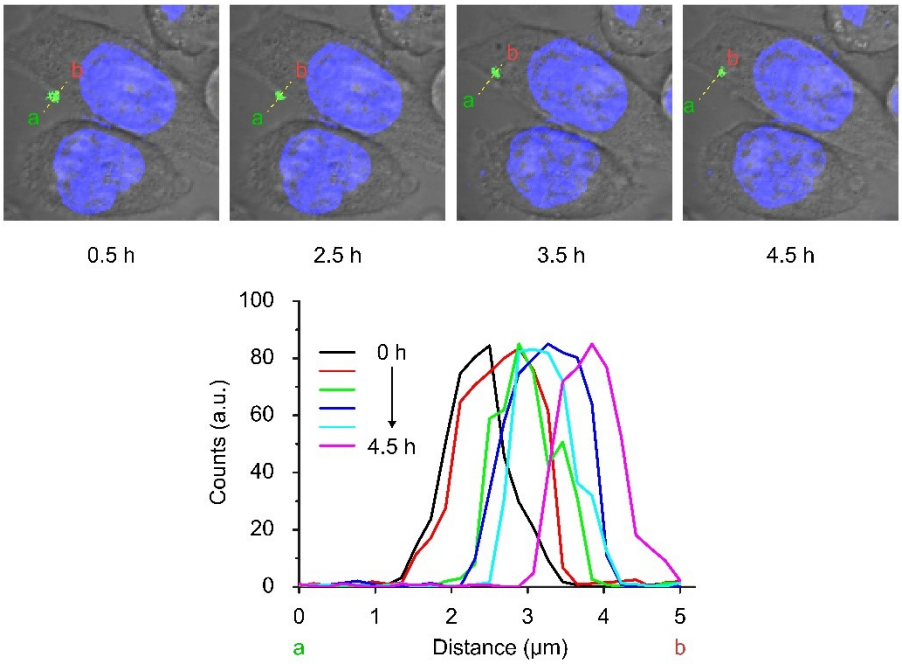

Figure S9. Cell internalization of coacervate protocells. **(A)** Time series of optical images demonstrating the approach of a coacervate protocell towards an individual living cell,

followed by electrostatic interaction mediated cell internalization. Scale bars, 5 μm. (**B**) Time- and spatial-dependent changes in the fluorescent profile and relative fluorescent peak intensities (a–b) on the white line shown in **(A)**.

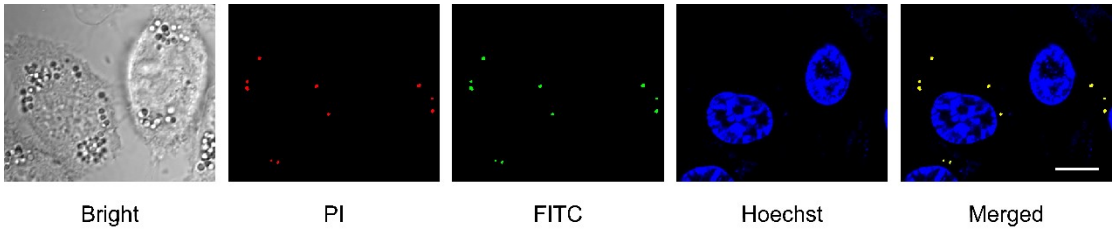

Figure S10. Fluorescence imaging of living cells after cellular internalization of coacervate protocells (2.5 h incubation). plasmid DNA was stained with PI (red) and DEAE–dextran was labelled with FITC (green). The nuclei of living cells were stained with Hoechst (blue). Scale bar: 10 μm.

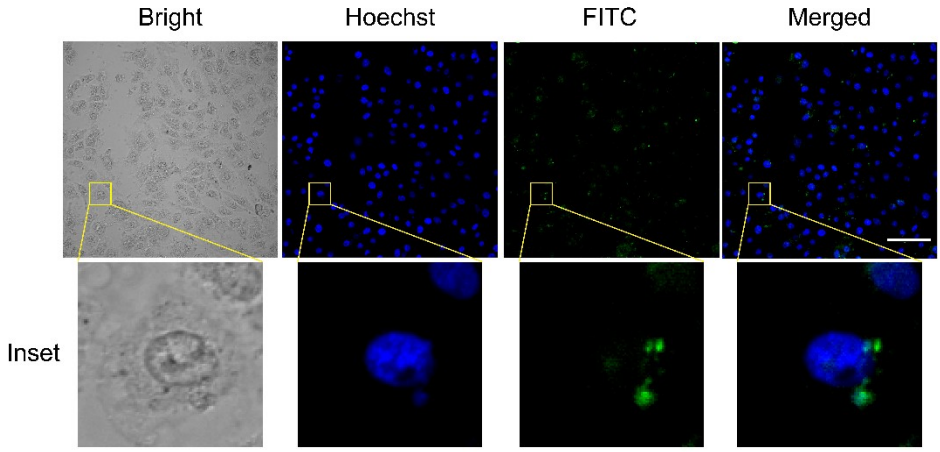

Figure S11. Coacervate protocells are located near the nucleus. Confocal micrographs of living cells after internalization of coacervate protocells for 6 h. Inset: an enlarged view of the yellow dotted square region in the imaging above by 8.57 times. The nuclei of living cell were stained with Hoechst. The coacervate protocells were doped with FITC-DEAE-dextran. Scale bars: 50 μm.

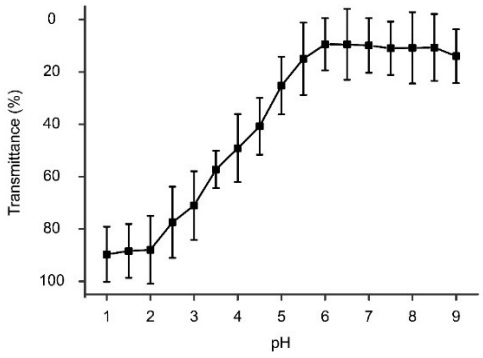

Figure S12. Transmittance determination of DEAE-dextran/PAA coacervates under different pH (1.0-9.0). DEAE-dextran/PAA coacervate: 5 mg·mL^{-1}.

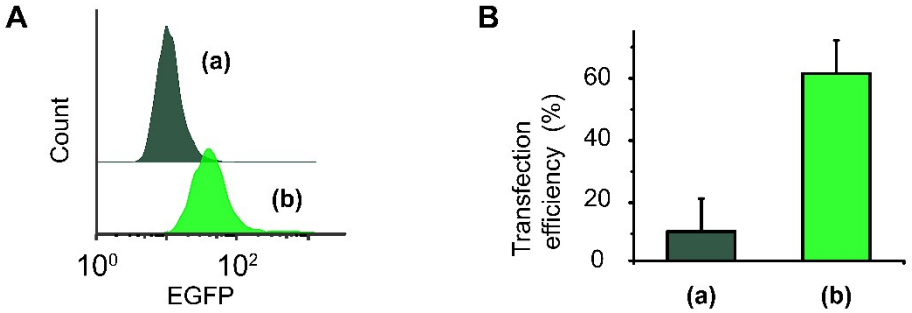

Figure S13. The flow analysis of pEGFP transfection and expression. **(A)** Histogram plot of the EGFP fluorescence in **Figure 2E**. (**B**) Transfection efficiency of (a) Free plasmid DNA and (b) Plasmid DNA in coacervate.

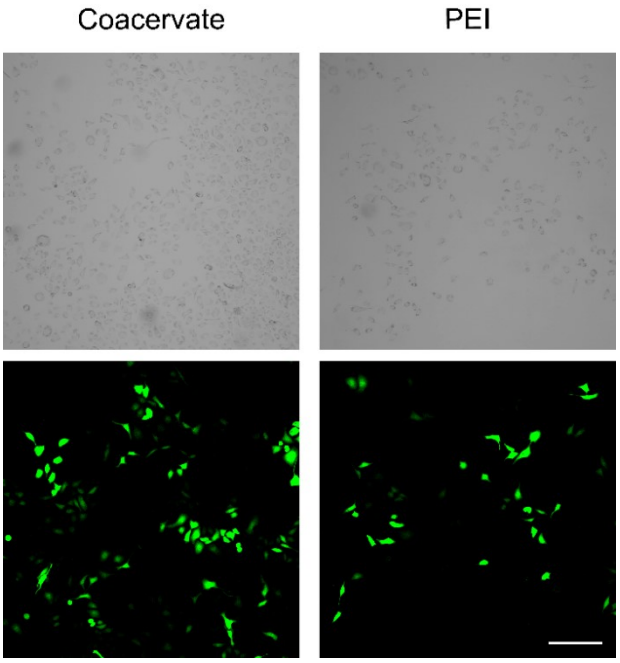

Figure S14. Confocal fluorescence images of green EGFP in cells transfected by coacervate and PEI. Scale bar: 100 μm. The concentration of coacervate microdroplets and PEI is 25 ug/mL.

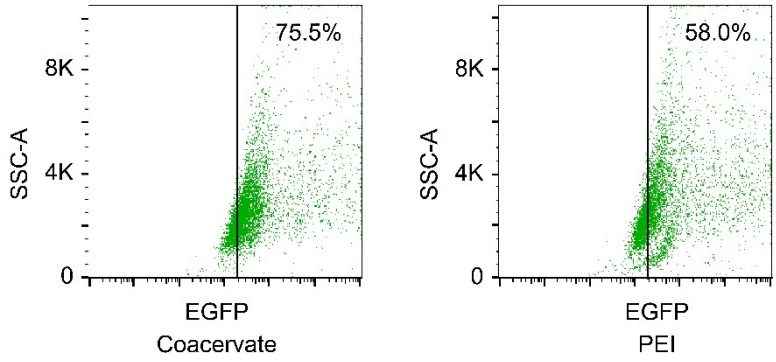

Figure S15. FACS 2D dot plots of EGFP fluorescence versus SSC signal in cells transfected by coacervate and PEI. The concentration of coacervate microdroplets and PEI is 25 ug/mL.

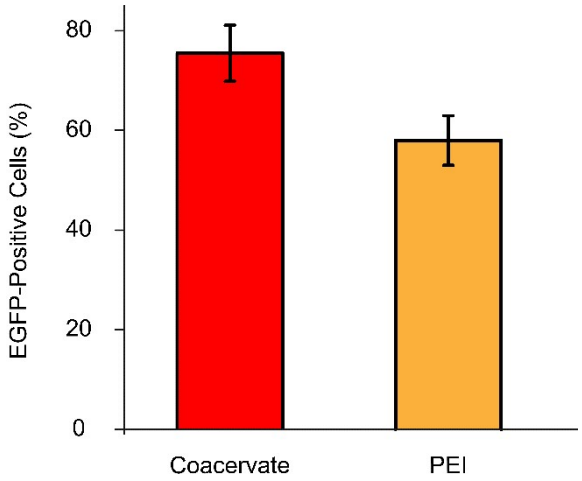

Figure S16. Proportion of EGFP-positive cells calculated using a flow cytometer in SMMC-7721 cells transfected with the complexes of pEGFP and different carriers (Coacervate, and PEI) (**p*<0.05).

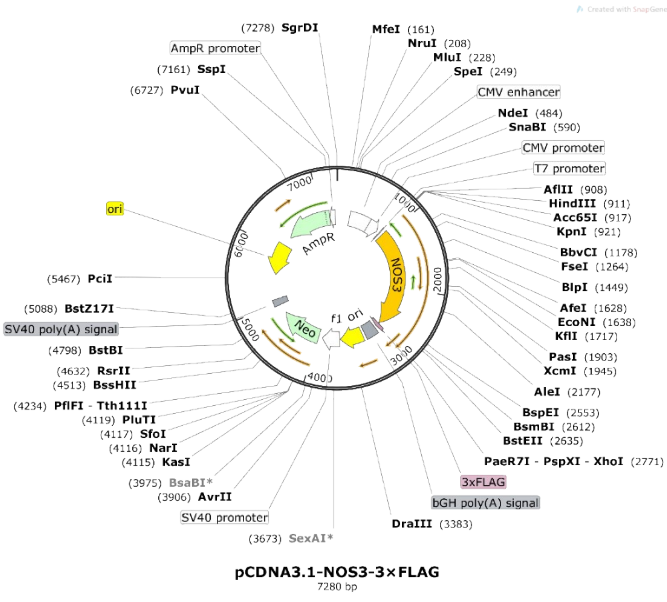

Figure S17. The plasmid profiles of pCDNA3.1-NOS3-3×FLAG.

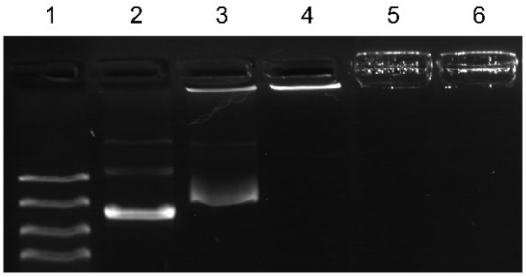

Figure S18. Agarose gel electrophoresis retardation assays of the pCDNA3.1-NOS3 loading in coacervate microdroplets. DNA marker (lane 1), free pNOS (lane 2), pNOS in coacervate with varying DEAE–dextran-PAA coacervate /pNOS weight ratios (0.02, 0.04, 0.06, 0.08, w/w, in lane 3-6, respectively.)

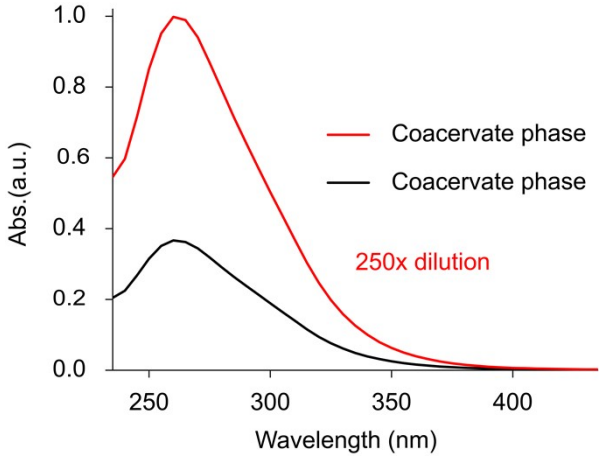

Figure S19. UV–Vis absorption spectra of pNOS in coacervate phase and supernatant continuous phase. UV–vis absorption of the pNOS in aqueous solution was monitored at 260 nm. Partition in the coacervate phase was ascertained after decomposition using 0.5 M NaCl at 250× dilution.

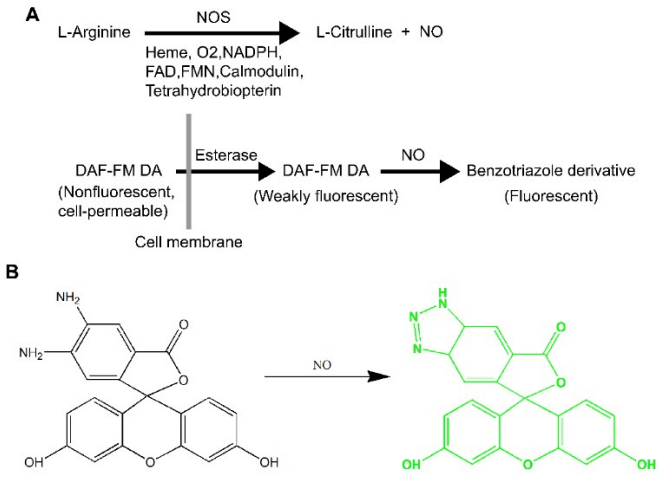

Figure S20. (A) Schematic diagram of nitric oxide synthase detection kit. (B) DAF-FM fluorescent assay for the determination of NO.

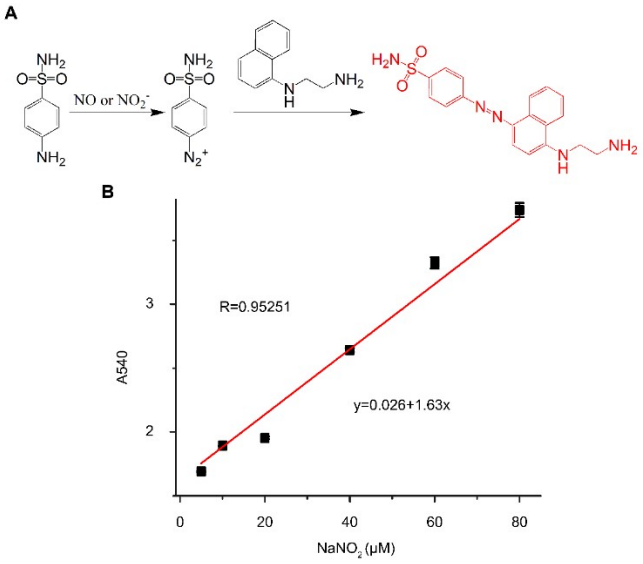

Figure S21. (A) Griess assay for the colorimetric determination of NO_2^- or NO. Nitric oxide metabolizes rapidly into nitrate and nitrite, which are stable. In NO assays, the nitrate is converted to nitrite, then assayed with Griess Reagent. (B) Standard curve line in total NO assay, $NaNO_2$ as standard nitrite.

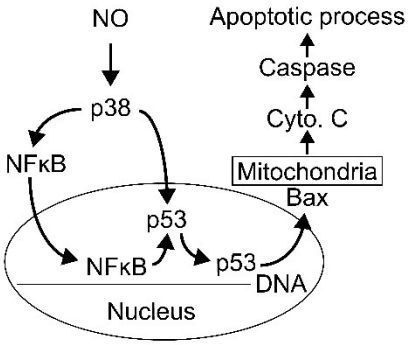

Figure S22. Schematic summary of cell apoptosis induced by NO. overproduction of NO activates caspase family proteases through the release of mitochondrial cytochrome C into the cytosol, upregulation of p53 expression, and alterations in the expression of apoptosis-associated proteins including the Bcl-2 family.

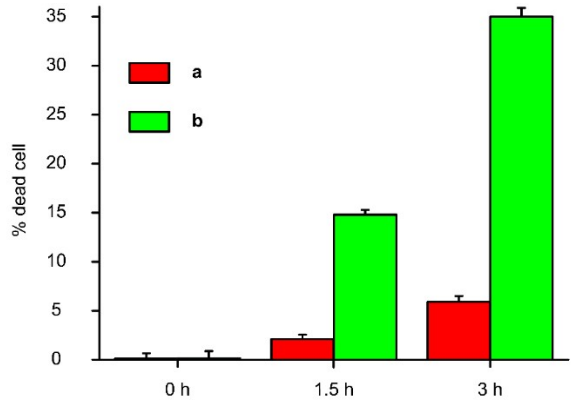

Figure S23. Quantification of cell number in Calcein-AM and PI staining assay for live/dead cells in **Figure 4A**. (a) Free pNOS and (b) pNOS in coacervate.

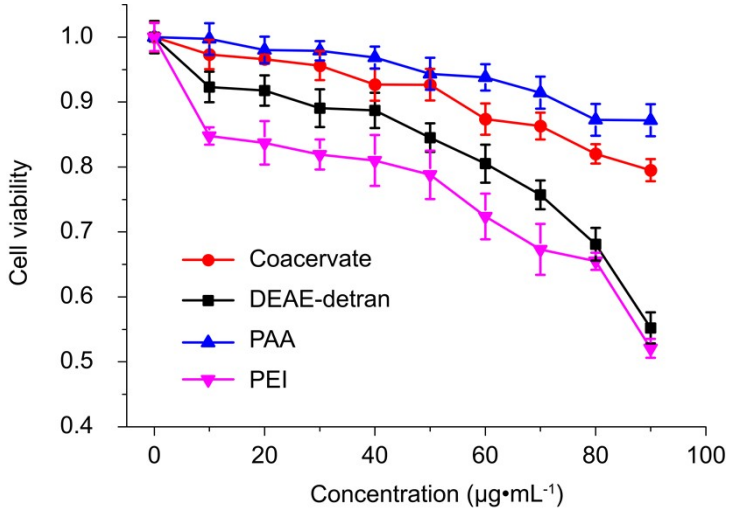

Figure S24. Relative cell viability data of SMMC-7721 cells incubated with different concentrations of DEAE-dextran/PAA coacervate (red), DEAE-dextran (black), PAA (blue) and PEI (pink) measured by the MTT cell viability assay. The incubation time was 24 h. Error bars were based on triplicated samples. The control samples of PEI or DEAE-dextran (10 mg/mL) were prepared though dissolving PEI and DEAE-dextran in deionized water, respectively and the final pH values were adjusted to pH = 7.0-9.0.

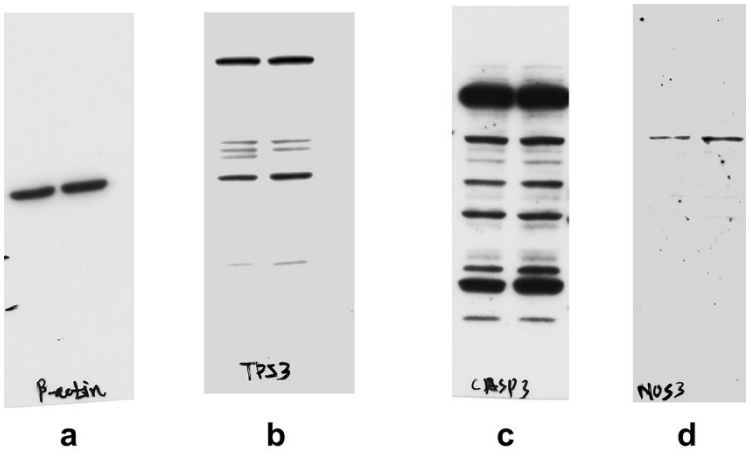

Figure S25. Full western blot images of protein levels of p53, Caspase-3 and NOS in SMMC-7721 cells transfected with (a) Free pNOS and (b) pNOS-coacervate.

References

(1) Vakaloglou, K. M.; Chrysanthis, G.; Rapsomaniki, M. A.; Lygerou, Z.; Zervas, C. G. IPP complex reinforces adhesion by relaying tension-dependent signals to inhibit integrin turnover. *Cell Rep.* **2016**, *14*, 2668-2682.

(2) Jönsson, P.; Jonsson, M. P.; Tegenfeldt, J. O.; Höök, F. A method improving the accuracy of fluorescence recovery after photobleaching analysis. *Biophys. J.* **2008**, *95*, 5334-5348.

(3) Bryan, N. S.; Grisham, M. B. Methods to detect nitric oxide and its metabolites in biological samples. *Free Radic. Biol. Med.* **2007**, *43*, 645-657.